Journal of the Korean Chemical Society
2010, *Vol. 54, No. 4*
Printed in the Republic of Korea
DOI 10.5012/jkcs.2010.54.4.402

2-Aminopyrimidine 및 2,4-Dihydoxybenzaldehyde 치환체인 Schiff-염기의 전이금속 착물에 대한 합성 및 특성 그리고 부식방지에의 응용

Abd El-Fatah M. Ouf, Mayada S. Ali, Mamdouh S. Soliman, Ahmed M. El-Defrawy, and Sahar I. Mostafa*
Chemistry Department, Faculty of Science, Mansoura University, Mansoura 35516, Egypt
(접수 2009. 6. 9; 수정 2009. 8. 4; 게재확정 2010. 5. 20)

Synthesis and Characterization of New Transition Metal Complexes of Schiff-base Derived from 2-Aminopyrimidine and 2,4-Dihydroxybenzaldehyde and Its Applications in Corrosion Inhibition

Abd El-Fatah M. Ouf, Mayada S. Ali, Mamdouh S. Soliman, Ahmed M. El-Defrawy, and Sahar I. Mostafa*
Chemistry Department, Faculty of Science, Mansoura University, Mansoura 35516, Egypt
**E-mail: sihmostafa@yahoo.com*
(Received June 9, 2009; Revised August 4, 2009; Accepted May 20, 2010)

요약. 새로운 착물인 *cis*-[Mo_2O_3(Hapdhba)$_2$], *trans*-[UO_2(Hapdhba)$_2$], [Pd(Hapdhba)Cl(H_2O)], [Pd(bpy)(Hapdhba)]Cl, [Ag(bpy)(Hapdhba)], [Ru(Hapdhba)$_2$(H_2O)$_2$], [Rh(Hapdhba)$_2$Cl(H_2O)] 및 [Au(Hapdhba)Cl_2]를 보고한다. 여기서 H_2apdhba는 2-aminopyrimidine 및 2,4-dihydoxybenzaldehyde에서 비롯된 Schiff-염기이다. 이들 착물은 IR, UV-Vis 그리고 질량 스펙트럼을 비롯하여 전기전도도, 자기 및 열 분석을 통해 특성을 조사하였다. 구리의 부식에 대한 H_2apdhba의 방해효과는 0.5 M HCl에서 potiodynamic polarization 측정을 통해 조사하였다.

주제어: Schiff-염기, H_2apdhba, 아조메틴, 스펙트럼, 편극

ABSTRACT. New complexes *cis*-[Mo_2O_5(Hapdhba)$_2$], *trans*-[UO_2(Hapdhba)$_2$], [Pd(Hapdhba)Cl(H_2O)], [Pd(bpy)(Hapdhba)]Cl, [Ag(bpy)(Hapdhba)], [Ru(Hapdhba)$_2$(H_2O)$_2$], [Rh(Hapdhba)$_2$Cl(H_2O)] and [Au(Hapdhba)Cl_2] are reported, where H_2apdhba is the Schiff-base derived from 2-aminopyrimidine and 2,4-dihydroxy benzaldehyde. The complexes were characterized by IR, electronic, ^{1}H NMR and mass spectra, conductivity, magnetic and thermal measurements. The inhibitive effect of H_2apdhba for the corrosion of copper in 0.5 M HCl was also determined by potentiodynamic polarization measurements.

Keywords: Schiff-base, H_2apdhba, Azomethine, Spectra, Polarization

INTRODUCTION

Schiff-bases are important class of ligands in coordination chemistry. They have a variety of applications in biology and analytical fields.[1] A large number of Schiff-base complexes have been studied because of their interest and important properties, e.g., their ability to reversibly bind oxygen,[2] catalytic activity,[3-5] transfer of amino groups,[6] complex formation ability towards toxic metal ions[7] and photo-chromic properties.[8]

This report is a continuation of our research program in the coordination chemistry of Schiff-base complexes. We have early reported the chemistry of Schiff-base derived from salicylaldehyde and 3-aminopropyltriethoxysaline complexes and their applications in catalytic epoxidation of olefins.[5] The interaction of Schiff-bases derived from 2-hydroxybenzaldehyde moiety and primary amines, especially amino acids with Ru(II), Mn(II), Mn(III), UO^{2+} and VO_2^+ have been reported.[4,9,10-12] It is known that, pyrimidine moeity is present in nucleic acids, several vitamins, coenzymes and antibiotics[13] and act as valuable substrates in the synthesis of antitumour agents.[14]

The most efficient acid inhibitors in cleaning solution for industrial equipments are organic compounds that mainly contain O, N, S and multiple bonds through which they are adsorbed on metal surface. Schiff-bases have great inhibition efficiency due to the presence of the azomethine (-N=C) group in the molecule.[15] Some Schiff-bases have been reported as corrosion inhibitors for steel, copper and aluminium.[15-17]

In this study, we have synthesized new complexes of Schiff- base derived from 2-aminopyrimidine and 2,4-dihydroxybenzaldehyde. These complexes have been charac-

terized on the bases of elemental analyses, spectral (IR, ^{1}H NMR, electronic and mass), conductivity, magnetic and thermal measurements. In addition, we report the inhibitive properties of H_2apdhba towards the corrosion of copper in acidic media using potentiodynamic polarization method.

EXPERIMENTAL SECTION

Materials

All manipulations were performed under aerobic conditions using materials and solvents as received. [Pd(bpy)Cl_2],[18] was synthesized as previously reported.

Elemental analyses (C, H, N, Cl) were performed by the Micro Analytical Unit of Cairo University. Magnetic moments at 25 ^{o}C were recorded using a Johnson Matthey magnetic susceptibility balance with Hg[Co(SCN)$_4$] as calibrant. IR spectra were measured as KBr discs on a Matson 5000 FT-IR spectrometer. Electronic spectra were recorded using a Unicam $UV_{2\text{-}100}$ U.V.-vis. Spectrometer. ^{1}H NMR spectra were measured on a Varian Gemini WM-200 spectrometer (Laser Centre, Cairo University). Thermal analysis measurements were made in the 20 - 800 ^{o}C range at the heating rate of 10 ^{o}C min^{-1}, using α-Al_2O_3 as a reference, on a Shimadzu Thermogravimetric Analyzer TGA- 50. Conductometric measurements were carried out at room temperature on a YSI Model 32 conductivity bridge. Mass spectra were recorded on a Matson MS 5988 and MS25RFA spectrometer. GAUSSIAN 03 program was used in the computational calculations.[19] The geometry optimization was carried out with the DFT method with the use of Becke-style three parameter functional[20] and Lee B3LYP functional.[21] The polarization measurements were carried out using AC signals of amplitude 10 mV peak to peak at open circuit potential in the frequency rang 10^{-5} Hz to 0.5 Hz by using Potentiostata/Galvanostata (Gamry PCI 300/4) and a personal computer with EIS 300 software for calculations.

Preparation of H_2apdhba

The Schiff-base, H_2apdhba, was synthesised by the condensation of ethanolic solutions of 2-aminopyrimidine (0.095 g, 1 mmol) and 2,4-dihydroxybenzaldehyde (0.138 g, 1 mmol) in presence of drops of glacial acetic acid. The orange product was filtered off during hot, washed with ethanol, diethyl ether and dried in *vacuo*. Elemental Anal. Calc. for $C_{11}H_9N_3O_2$: C, 61.4; H, 4.2; N, 19.5%. Found C, 61.3; H, 4.2; N, 19.0%. IR: ν (CH=N), 1622; ν (C=N), 1560; ν (C=C), 1575; ν (C-O), 1229 cm^{-1}. ^{1}H NMR: 9.94 (CH=N, s), 7.32 (H (3), s); 6.57 (H (5), d); 7.55 (H (6), d); 8.22 (H (4',6'), d); 8.80 (H (5'), t) ppm. Mass spectrum, m/z: 216 (MH^+), 136 (M^+ - $C_4H_3N_2$).

Preparation of the complexes

***cis*-[Mo_2O_5(Hapdhba)$_2$].H_2O:** An aqueous solution (5 cm^3) of ammonium molybdate (0.116 g, 0.5 mmol) was added to ethanolic solution (15 cm^3) of H_2apdhba (0.107 g, 0.5 mmol). The reaction mixture was heated under reflux for 2 h. The pale orange precipitate was filtered off, washed with ethanol, diethyl ether and dried *in vacuo*. Conductivity data (10^{-3} M in DMSO) : Λ_M = 4.0 ohm^{-1} cm^2 mol^{-1}. Elemental Anal. Calc. for $C_{22}H_{18}Mo_2N_6O_{10}$: C, 36.8; H, 2.5; N, 11.7%. Found C, 36.6; H, 2.5; N, 11.5% IR: ν (CH=N) 1605; ν (C=N) 1559; ν (C=C) 1578; ν (C-O) 1241; ν_s(MoO_2) 926; ν_{as}(MoO_2) 901; ν (Mo_2O) 745cm^{-1}. ^{1}HNMR: 10.06 (CH=N, s); 7.50 (H(3), s); 6.60 (H(5), d); 7.59 (H(6), d); 8.23 (H (4',6'), d); 8.82 (H (5'), t) ppm. UV-Vis (in DMSO): λ_{max} 450, 360 nm. Mass spectrum, *m/e*: 719 [Mo_2O_5(Hapdhba)$_2$]$^+$, 489 [Mo_2O_5 (Hapdhba)]$^+$, 273 [Mo_2O_5]$^+$.

***trans*-[UO_2(Hapdhba)$_2$]:** $UO_2(NO_3)_2.6H_2O$ (0.25 g, 0.5 mmol) in methanol (10 cm^3) was added to H_2apdhba (0.107 g, 0.5 mmol) in methanol (15 cm^3). The yellow mixture was heated under reflux for 4 h on a steam bath. Upon reducing the volume, a reddish brown complex was separated out, washed with methanol and dried *in vacuo*. Conductivity data (10^{-3} M in DMSO): Λ_M = 3.0 ohm^{-1} cm^2 mol^{-1}. Elemental Anal. Calc. for $C_{22}H_{16}N_6O_6U$: C, 37.8; H, 2.3; N, 12.0%. Found C, 37.6; H, 2.4; N, 11.9%. IR: ν (CH=N) 1603; ν (C=N) 1563; ν (C=C) 1560; ν (C-O) 1238; ν_{as}(UO_2) 925cm^{-1}. UV-Vis (in DMSO): λ_{max} 436, 410 nm.

[Pd(Hapdhba)Cl(H_2O)].H_2O: K_2PdCl_4 (0.163 g, 0.5 mmol) in water (5 cm^3) was added to H_2apdhba (0.107 g, 0.5 mmol) in ethanol (15 cm^3). The mixture was warmed and stirred for 12 h till a pale brown precipitate isolated, washed with ethanol and dried *in vacuo*. Conductivity data (10^{-3} M in DMSO): Λ_M = 8.0 ohm^{-1} cm^2 mol^{-1}. Elemental Anal. Calc. for $C_{11}ClH_{12}N_3O_4Pd$: C, 33.7; H, 3.1; N, 10.7; Cl, 9.1; Pd, 27.2%. Found C, 33.7; H, 3.0; N, 10.4; Cl, 9.0; Pd, 27.0%. IR: ν (CH=N) 1610; ν (C=N) 1561; ν (C=C) 1574; ν (C-O) 1241; ν (Pd-O) 540; ν (Pd-N) 435; ν (Pd-Cl) 328cm^{-1}. ^{1}HNMR: 10.08 (CH=N, s); 4.47 (H (3), s); 6.63 (H (5), d); 7.58 (H (6), d); 8.23 (H (4',6'), d); 8.84 (H(5'), t) ppm. UV- Vis (in DMF): λ_{max} 482, 380 nm. Mass spectrum, *m/e*: 393 [PdCl(H_2O) (Hapdhba)]$^+$, 337 [Pd(H_2O)(Hapdhba)]$^+$, 318 [Pd(Hapdhba)]$^+$.

[Pd(bpy)(Hapdhba)]Cl.H_2O: H_2apdhba (0.107 g, 0.5 mmol) was dissolved in methanolic solution of KOH (0.056 g, 1 mmol; 15 cm^3) and [Pd(bpy)Cl_2] (0.17 g, 0.5 mmol) was added. The mixture was heated with stirring for 10 h till a brown precipitate was isolated. It was filtered off, washed

with methanol, diethyl ether and dried *in vacuo*. Conductivity data (10^{-3} M in DMSO): Λ_M = 89.0 ohm^{-1} cm^2 mol^{-1}. Elemental Anal. Calc. for $C_{21}ClH_{18}N_5O_3Pd$: C, 47.6; H, 3.4; N, 13.2; Cl, 6.7; Pd, 20.1%. Found C, 47.7; H, 3.5; N, 13.5; Cl, 6.9; Pd, 20.0%. IR: ν (CH=N) 1608; ν (C=N) 1558; ν (C=C) 1579; ν (C-O) 1245; ν (Pd-O) 536; ν (Pd-N) 412 cm^{-1}. ^{1}HNMR: 10.05 (CH=N, s); 6.59 (H (5), d); 8.83 (H (5'), t) ppm. UV-Vis (in DMF): λ_{max} 476, 384 nm.

[Ag(bpy)(Hapdhba)]: $AgNO_3$ (0.085 g, 0.5 mmol) in water (1 cm^3) was added to bpy (0.078, 0.5 mmol) in ethanol (30 cm^3) to produce a solution of $[Ag(bpy)(H_2O)_2](NO_3)$ to which H_2apdhba (0.107 g, 0.5 mmol) was added. The reaction mixture was warmed in the dark for 8 h to produce a precipitate. It was filtered off, washed with methanol, diethyl ether and dried *in vacuo*. Conductivity data (10^{-3} M in DMSO): Λ_M = 1.0 ohm^{-1} cm^2 mol^{-1}. Elemental Anal. Calc. for $AgC_{21}H_{16}N_5O_2$: C, 52.7; H, 3.3; N, 14.7%. Found C, 52.3; H, 3.2; N, 14.8%. IR: ν (CH=N) 1609; ν (C=N) 1557; ν (C=C) 1581; ν (C-O) 1248; ν (Ag-O) 525; ν (Ag-N) 400 cm^{-1}. UV-Vis (in DMSO): λ_{max} 445, 360 nm.

[Ru(Hapdhba)$_2$(H$_2$O)$_2$].2H$_2$O: Hydrated ruthenium trichloride (0.051 g, 0.25 mmol) in ethanol (5 cm^3) was added to H_2apdhba (0.107 g, 0.5 mmol) in ethanol (15 cm^3). The brown solution was kept under reflux for 3 h and 5ml of 5M AcONa was added. The reaction mixture was refluxed for 3 h more till brown-violet microcrystals formed, washed with ethanol and dried *in vacuo*. Conductivity data (10^{-3} M in DMSO): Λ_M = 3.0 ohm^{-1} cm^2 mol^{-1}. Elemental Anal. Calc. for $C_{22}H_{24}N_6O_8Ru$: C, 43.9; H, 4.0; N, 14.0%. Found C, 44.0; H, 3.8; N, 13.6%. IR: ν (CH=N) 1611; ν (C=N) 1557; ν (C=C) 1563; ν (C-O) 1247; ν (Ru-O) 500; ν (Ru-N) 428 cm^{-1}. ^{1}HNMR: 10.04 (CH=N, s); 7.45 (H (3), s); 6.61 (H (5), d); 7.58 (H(6), d); 8.23 (H(4',6'), d); 8.85 (H(5'), t) ppm. UV-Vis (in DMSO): λ_{max} 540, 390, 330 nm. Mass spectrum, *m*/*e*: 603 $[Ru(H_2O)_2(Hapdhba)_2]^+$, 531 $[Ru(Hapdhba)_2]^+$, 318 $[Ru(Hapdhba)]^+$.

[Rh(Hapdhba)$_2$(H$_2$O)Cl].3H$_2$O: Rhodium trichloride (0.12 g, 0.45 mmol) was added to an aqueous solution of AcONa (0.62 g, 7.5 mmol; 30 cm^3). The mixture was heated gently with stirring under reflux and solid H_2apdhba (0.107 g, 0.5 mmol) was added in small portions. The reaction mixture was refluxed for 12 h and a reddish brown precipitate produced, which removed during hot, washed with hot water and air-dried. Conductivity data (10^{-3} M in DMSO) : Λ_M = 5.0 ohm^{-1} cm^2 mol^{-1}. Elemental Anal. Calc. for $C_{22}ClH_{24}N_6O_8Rh$: C, 41.3; H, 3.8; N, 13.2; Cl, 5.6%. Found C, 41.9; H, 3.8; N, 13.3; Cl, 5.6 %. IR: ν (CH=N) 1612; ν(C=N) 1560; ν (C=C) 1557; ν (C-O) 1245; ν (Rh-O) 520; ν(Rh-N) 455; ν (Rh-Cl) 330cm^{-1}. ^{1}HNMR: 10.00 (CH=N, s); 7.40 (H(3), s); 6.64 (H(5), d); 7.62 (H(6), d); 8.24 (H(4',6'), d); 8.85 (H(5'), t) ppm. UV-Vis (in DMSO): λ_{max} 590, 500 , 393 nm. Mass spectrum, *m*/*e*: 640 $[Rh(H_2O)Cl(Hapdhba)_2]^+$, 551 $[Rh(H_2O)(Hapdhba)_2]^+$, 532 $[Rh(Hapdhba)_2]^+$, 315 $[Rh(Hapdhba)]^+$.

[Au(Hpadhba)Cl$_2$].H$_2$O: Similar procedure as the rhodium analogue was applied, $HAuCl_4$ replacing $RhCl_3$ to produce brown precipitate. Conductivity data (10^{-3} M in DMSO): Λ_M = 8.0 ohm^{-1} cm^2 mol^{-1}. Elemental Anal. Calc. for $AuC_{11}Cl_2H_{10}N_3O_3$: C, 26.4; H, 2.0; N, 8.4; Cl, 14.2%. Found C, 26.2; H, 2.4; N, 8.7; Cl, 14.0%. IR: ν (CH=N) 1616; ν (C=N) 1563; ν (C=C) 1574; ν (C-O) 1248; ν (Au-O) 528; ν (Au-N) 443; ν (Au-Cl) 321cm^{-1}. ^{1}HNMR: 10.05 (CH=N, s); 7.42 (H(3), s); 6.61 (H(5), d); 7.59 (H(6), d); 8.25 (H(4',6'), d); 8.84 (H(5'), t) ppm.

Electrochemical polarization method

Cylindrical wire of copper (99.74% purity) was used as working electrode. The role was sealed to a glass tube with Araldite. The electrodes were ground to 600-grit finish, rinsed with water, degreased in alkaline mixture washed with bidistilled water and finally dried. This insured constant cross-sectional area would be exposed to the solution through the experiments. The exposed area was polished with different emery papers in the normal way starting from coarser to finer followed by ultrasonically degreasing in alkaline solution and finally washing with bidistilled water, just before insertion in the electrolytic cell.[15]

The electrochemical measurments were carried out using pure copper thin, dipped on 0.5 M HCl in present and absence of H_2apdhba. The working electrode was the pure copper thin sheet rod embedded with an exposed area of 0.5 cm^2. A rectangular platinum foil was used as the counter electrode. The area of the counter electrode was much larger compared to the area of the working electrode. This will exert an uniform potential field on the working electrode. Saturated calomel electrode (SCE) was used as reference electrode.[15]

In the polarization cell, 100 cm^3 of H_2apdhba (3×10^{-6}, 5×10^{-6} , 7×10^{-6} , 9×10^{-6} molL^{-1}) was used. The working electrode was polished with a fine grade emery papers and followed by ultrasonically degreasing with alkaline solution. The working and the reference electrodes were assembled and necessary connections were made with the instrument. A time interval of about 30 minutes was given for the system to attain a steady state and the open circuit potential (OCP)

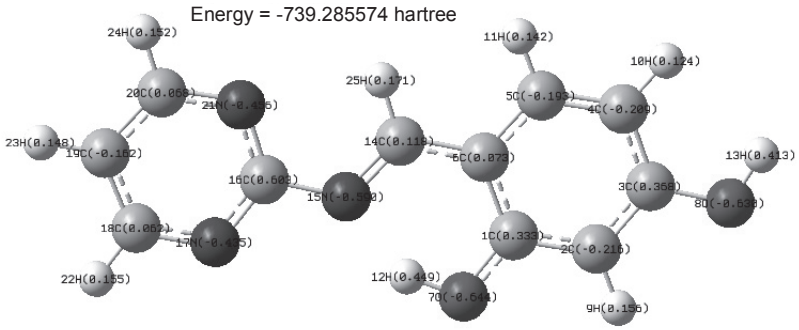

Conformation I (*cis* 2-OH to HC=N)

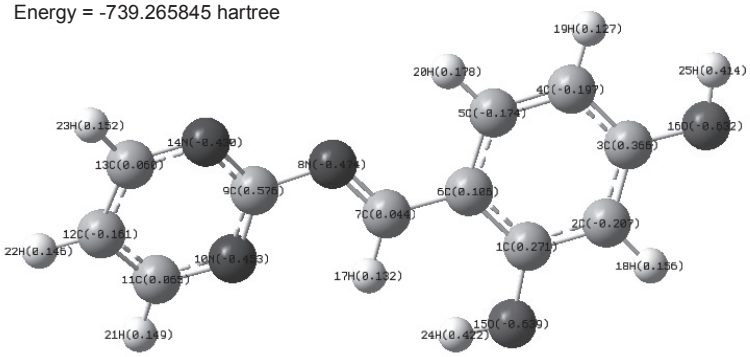

Conformation II (*trans* 2-OH to HC=N)

***Fig*. 1.** *cis* and *trans* Conformations of H_2apdhba.

***Table* 1.** Selected bond lengths (Å) and bond angles (°) of H_2apdhba, using the B3LYP/6-31G (d) level of DFT (see *Fig*. 1 for numbering Scheme)

Bonds	Bond lengths (Å)
C(6) - O(7)	1.334 Å
C(6) - C(14)	1.435 Å
C(14) - H(25)	1.094 Å
C(14) - N(15)	1.301Å
C(16) - N(15)	1.397 Å
C(16) - N(17)	1.345 Å
C(16) - N(21)	1.346 Å
O(7) - H(12)	1.005Å

was noted. The potentiodynamic current-potential curves were recorded by changing the electrode potential automatically from -1500 to 500 mV with scanning rate 5 mVs^{-1}. All the experiments were carried out at 25 ± 1 °C using ultra circulating thermostat.

RESULTS AND DISCUSSION

The experimental section lists some new complexes of Schiff-base derived from 2-aminopyrimidine and 2,4-dihydroxybenzaldehyde (H_2apdhba). The elemental analyses of the isolated complexes agree with the assigned formulae. The molar conductivities (Λ_M) in DMSO at room temperature showed all the complexes to be non-electrolytes except the complex [Pd(Hapdhba)(bpy)]Cl, which is (1:1) electrolyte.[22] The complex $[Mo_2O_5(Hapdhba)_2]$ was prepared by the reaction of H_2apdhba with $[MoO_4]^{2-}$ in aqueous ethanol. *Trans*-$[UO_2(Hapdhba)_2]$ was obtained by the reaction of uranyl nitrate and H_2apdhba in methanol. The complex $[Pd(Hapdhba)Cl(H_2O)]$ made from K_2PdCl_4 and H_2apdhba in aqueous ethanol while [Pd(bpy)(Hapdhba)]Cl was made from $[Pd(bpy)Cl_2]$ and H_2apdhba in potassium methoxide. [Ag(bpy)(Hapdhba)] was isolated from the reaction of H_2apdhba and $[Ag(bpy)(H_2O)_2]NO_3$ in H_2O-MeOH in the dark. The complexes $[Ru(Hapdhba)(H_2O)_2]$, $[Rh(Hapdhba)_2(H_2O)Cl]$ and $[Au(Hapdhba)Cl_2]$ were obtained from the reflux of hydrated $RuCl_3$, $RhCl_3$ or $HAuCl_4$ and excess of H_2apdhba

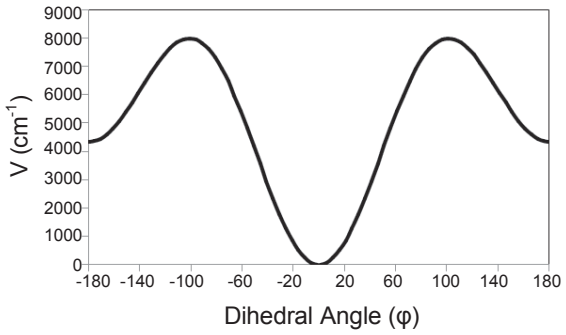

***Fig*. 2.** Potential energy function governing the conformational interchange of H_2apdhba.

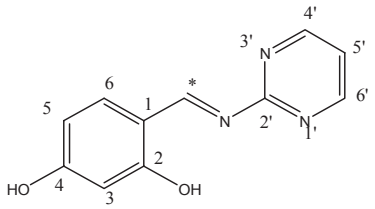

***Fig*. 3.** Structure of H_2apdhba

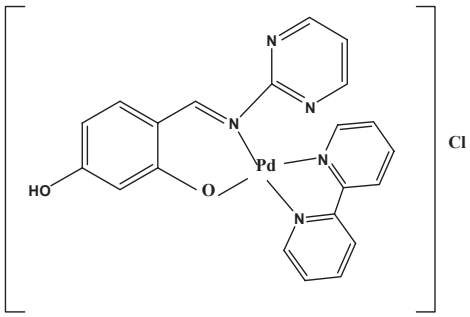

***Fig*. 4.** Complex [Pd(bpy)(Hpadhba)]Cl

under basic conditions.

A point of synthetic interest is the fact that the sequences of reagent addition in most procedures are critical. The complexes are microcrystalline or powder-like, stable in the normal laboratory atmosphere and partially soluble in DMF and DMSO. We had hoped to structurally characterize one of the complexes by single X-ray crystallography, but were thwarted on numerous occasions by very small crystal dimensions. Thus, the characterization of these complexes was based on physical and spectroscopic techniques.

Computational details

DFT calculations were performed with the GAUSSIAN 03 program package.[19] The geometry of the Schiff-base, H_2-apdhba, was optimised by the DFT method with the B3LYP functional.[20,21] The optimized geometrical parameters of H_2-apdhba are gathered in *Table* 1. *Fig*. 1 shows that the aromatic and pyrimidine rings are nearly planar to each others. Also, The conformation I (*cis*, 2-OH to N=CH) is more stable than conformation II (*trans*, 2-OH to N=CH) and the energy difference $\Delta E = 12.4$ Kcalmol^{-1} (4330 cm^{-1}). The potential function governing the conformational interchange between the two conformers is observed in *Fig*. 2. Also, the calculated charge densities on the active centers showed that the oxygen (2-OH) and nitrogen (N=CH) centers are the accessible for interaction with the metal (without interaction from the pyrimidine cyclic nitrogen and 4-OH centers). The calculated charge densities contour values indicated that these two centers having the highest charge densities in the molecule (The N- atom of the N=CH group has high charge density comparable to the pyrimidine ring cyclic nitrogen centers). Moreover, the spacing distance between the hydrogen of 2-OH and nitrogen of N=CH is 1.713 Å, i.e., may leave the 2-OH group free.

Infrared spectra

The solid-state properties of the Schiff-base (H_2apdhba, *Fig*. 3) were examined by IR spectroscopy. The spectrum was compared with those of the complexes. Tentative assignments of selected IR bands are reported in the experimental section. The spectrum of H_2apdhba exhibits a strong band at 1622 cm^{-1} which is characteristic of ν (HC=N) group. It is expected that coordination of the nitrogen centre to the metal ion would reduce the electron density in the azomethine link and thus shifted the ν (HC=N) to lower wave numbers.[3] In the IR spectra of the complexes, this band is shifted to the region at 1605 - 1612 cm^{-1}.[3,23] An intense band at 1229 cm^{-1} in the free H_2apdhba has been assigned to the phenolic ν (C-O) stretch. In complexes, this band is shifted to higher frequencies, indicating the coordination of H_2apdhba through the deprotonated phenolic (C_2-O$^-$).[24] These data has been further supported by the disappearance of the broad band at 3387 cm^{-1} attributed to ν (2-OH); the deprotonation occurs prior to coordination. The band at 3217 cm^{-1} in the H_2apdhba due to ν (4-OH) stretch is unaffected by coordination.[11] In the free H_2apdhba, strong bands at 1575 and 1560 cm^{-1}, attributed to the non-aromatic pyrimidine ring ν (C=C) and ν (C=N) stretches, respectively,[14] are not affected upon complexation. This feature was expected from the DFT quantum calculations.

Also, in the spectra of [Pd(bpy)(Hapdhba)]Cl (*Fig*. 4) and [Ag(bpy)(Hapdhba)], the bands near 1628, 1590, 1505, 1475 and 1420 cm^{-1} are attributed to the bpy stretching vibrations;[25]

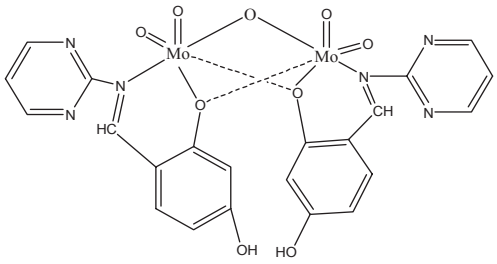

***Fig*. 5.** Complex $[Mo_2O_5(Hapdhba)_2]$

these bands are shifted to higher compared with the free bpy indicating its participation in complexation. The bands at 854, 841, 743 and 725 cm^{-1} are assigned to the *v* (CH) vibrations of the coordinated bpy.[26]

In the 1000-750 cm^{-1} region, the spectrum of $[Mo_2O_5(Hapdhba)_2]$ (*Fig*. 5) shows bands characteristic of the *cis*-MoO_2^{2+} units and the $\{O_2Mo\text{-}O\text{-}MoO_2\}^{2+}$ core.[27] The IR bands at 926 and 901 cm^{-1} are assigned to the $\nu_s(MoO_2)$ and $\nu_{as}(MoO_2)$ modes, respectively. The appearance of two stretching bands is indicative of the *cis* configuration.[26] The strong IR band at 745 cm^{-1} is assigned to the ν_{as}(Mo-O-Mo) mode indicating the presence of a $\mu\text{-}O^{2-}$ group.[26] The IR spectrum of $[UO_2(Hapdhba)_2]$ exhibits only one U=O stretching band, *i.e.* $\nu_{as}(UO_2)$, at 925 cm^{-1} indicating its linear *trans*-dioxo configuration.[28] The $\nu_s(UO_2)$ mode appears as a very weak peak at 909 cm^{-1}.[29]

The region of the complex spectra between 520 and 200 cm^{-1} contains several weak bands; these may assign to ν (M-O), ν (M-N) and ν (M-Cl) stretches, respectively.[27-29]

^{1}H NMR spectra

The ^{1}H NMR assignments of H_2apdhba and some of the representative complexes (in DMSO-d_6) are listed in the experimental section. The ^{1}H NMR spectrum of the free H_2apdhba exhibits a triplet at δ 8.80 ppm and two singlets at δ 9.94 and 7.30 ppm and four doublets at δ 6.60, 7.50, 8.22 and 8.22 ppm: these probably arise from H(5'), CH=N, H(3), H(5), H(6), H(4') and H(6'), respectively (see *Fig*. 3 for numbering scheme). The protons of the hydroxy groups appear as broad singlets at δ 12.20 (2-OH) and 11.01 (4-OH) ppm.[30] In the ^{1}H NMR spectra of the complexes, the resonance arising from the hydroxyl (2-OH) proton is not observed, indicating the replacement of the hydroxyl proton by the metal ion.[30] The signal due to the azomethine proton (-HC=N) is found to be considerably deshielded δ > 10.05 ppm relatively to that of the free H_2apdhba (δ = 9.94 ppm) as a consequence of electron donation to the metal centre.[31,32] The resonance arising from H(3) and H(6) shift to higher field to a great extent than the others, probably owing to a decrease in the electron density in the aromatic ring more than the pyrimidine one upon complexation.[30]

In the ^{1}H-NMR spectrum of $[Pd(bpy)Cl_2]$, the bpy protons experience downfield shifts as compared to the free bpy protons.[25] In the ^{1}H-NMR spectra of [Pd(bpy)(Hapdhba)]Cl, the bpy shows upfield shifts as compared with $[Pd(bpy)Cl_2]$. This is interpreted in terms of stronger binding of $Hpadhba^-$ to Pd(II) as compared to binding of chloride ion.[33] The ^{1}H-NMR spectrum of [Pd(bpy)(Hapdhba)]Cl shows complicated multiplet in δ 7.1 - 8.4 ppm region are assigned to the bpy protons that interfere with the aromatic (H_2apdhba) protons resonances.

Electronic Spectra

The solution electronic spectra of H_2apdhba complexes were recorded in DMSO and EtOH in the 200 - 800 nm range. Transition below 400 nm are assigned to intra-ligand charge transfer ($n \rightarrow \pi^*$) and ($\pi \rightarrow \pi^*$). The electronic spectra of the complexes contain intense bands due to ligand to metal charge transfer (LMCT) and weaker bands assigned to d-d transitions.[34]

The electronic spectrum of the diamagnetic $[Rh(Hapdhba)_2Cl(H_2O)]$ complex displays bands at 590, 500 and 393 nm which resemble those of other six-coordinate Rh(III) complexes and may assign to $^1A_{1g} \rightarrow {}^3T_{1g}$, $^1A_{1g} \rightarrow {}^1T_{1g}$ and $^1A_{1g} \rightarrow {}^1T_{2g}$ transitions, respectively.[26,35]

The electronic spectrum of the diamagnetic $[Ru(Hapdhba)_2(H_2O)_2]$ complex shows high intense transition at 540 ($^1A_{1g} \rightarrow {}^1T_{1g}$), 390 ($^1A_{1g} \rightarrow {}^1T_{2g}$) and 330 (ligand ($\pi\text{-}d\pi$)) nm.[26,35] This feature is attributed to a low-spin octahedral geometry around Ru(II). Similar spectral data are reported for $[Ru(YPh_3)_2(Hcdhp)_2]$ (Y = P, As, Hcdhp = 5-chloro-3-hydroxy-2-pyridinone)complexes[35] and $[Ru(PPh_3)_2(apc)_2]$ (ap = 3-aminopyrazine-2-carboxylic acid).[26]

In the electronic spectrum of $[Mo_2O_5(Hapdhba)_2]$, $[MoO_2]^{2+}$ displays bands at 450 and 360 (shoulder) nm, the later band is assigned to $O^{2-} \rightarrow Mo^{VI}$ (p-d transition) and is characteristic of the MoO_2^{2+} moiety in octahedral geometry.[5]

The electronic spectrum of *trans*-$[UO_2(Hapdhba)_2]$ shows two bands at 463 and 410 nm may be due to $\Sigma_g^{1+} \rightarrow {}^2\pi_u$ and $n \rightarrow \pi^*$ charge transfer, respectively.[33,35]

the electronic spectrum of [Ag(bpy)(Hapdhba)] shows bands at 445 and 360 nm; the latter one may arise from charge transfer of the type ligand (π) $\rightarrow b_{1g}$ (Ag^+) and ligand (σ) $\rightarrow b_{1g}$ (Ag^+), respectively, in a typical distorted square planar environment around the metal ion.[14]

The electronic spectra of the diamagnetic palladium(II) complexes show square planar environment around Pd(II).

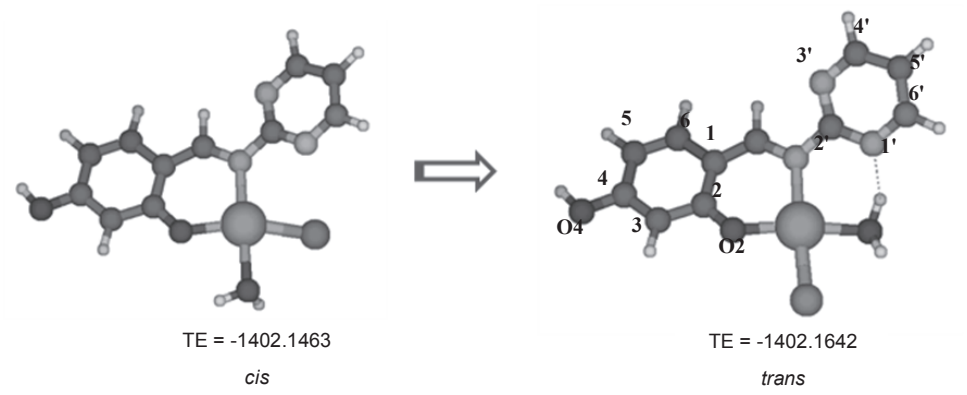

***Fig*. 6.** *cis* and *trans* Conformations of [Pd(Hapdhba)Cl(H_2O)]

***Table* 2.** The optimized bond lengths and angles, and atomic charges of [Pd(Hapdhba)Cl(H_2O)]. (see *Fig*. 6 for numbering Scheme)

Bond	Bond Lengths (Å)	Bond Angles	Angle (°)	Atom	Charge
Pd-O_{H2O}	2.095	Cl-Pd-O_{H2O}	83.42	Pd	0.863
Pd-Cl	2.345	N-Pd-O_{H2O}	95.21	Cl	-0.557
Pd-$N_{N=CH}$	2.113	Cl-Pd-O(2)	89.09	O (H_2O)	-0.968
Pd-O(2)	1.997	N-Pd-O(2)	92.48	O(2)	-0.618
CH=N	1.330			O(4)	-0.690
C(1)-C(2)	1.451			N(CH=N)	-0.581
C(2)-O(2)	1.288			N(1')	-0.555
C(1)-$C_{CH=N}$	1.405			N(3')	-0.520
C(4)-O(4)	1.361				
N(1')-C(2')	1.351				
C(2')-N(3')	1.346				
N(1')-C(6')	1.339				
N(3')-C(4')	1.330				

In the visible region, three spin-allowed singlet-singlet d-d transitions are predicted.[14,33] The ground state is $^1A_{1g}$ and the excited states corresponding to three transitions are $^1A_{2g}$, $^1B_{1g}$ and ^1E_g in order of increasing energy. Strong charge transfer transitions interfere and prevent the observation of the expected bands. The absorption band near 380 nm is assigned to combination of charge transfer transition from palladium d-orbital to π* orbital of 2,2'-bipyridyl and d-d bands while the band near 475 nm due to a combination of ligand (π) to metal charge transfer and M(II) d-d bands.[35]

Geometry optimisation of [Pd(Hapdhba)Cl(H_2O)]

The geometry of [Pd(Hapdhba)Cl(H_2O)] was optimized in a single state by the DFT method with the B3LYP functional. Two geometrical isomers are available; *cis* and *trans* oxygen conformations (O(2) from Hapdhba and O from coordinated H_2O) (*Fig*. 6). The intra-molecular hydrogen bonding between N1' (pyrimidine) and H (in coordinated H_2O) stabilizes the *trans* one.

The optimized geometry parameters are reported in *Table* 2. The calculated charge on the palladium atom (0.863) is considerable lower than the formal charge +2. It may come from the charge donation from the water oxygen, chloride and Hapdhba ligands. The charges on Cl and Hapdhba {O(2) and N=CH} are significantly smaller than -1 (for both). This feature confirms the higher electron density delocalization from the donor atoms to Pd(II) centre.

Thermal analysis

The thermal decomposition of the complexes, [Mo_2O_5(Hapdhba)$_2$].H_2O, [Pd(Hapdhba)Cl(H_2O)].H_2O and [Pd(bpy)(Hapdhba)]Cl.H_2O was studied using thermo-gravimetric (TG) technique. The weight loss observed below 150 °C is due to dehydration as colours changed from pale to deep.[11] The thermogram of [Mo_2O_5(Hapdhba)$_2$].H_2O shows the first step weight loss of 2.8% between 31 and 138 °C, which corresponds almost exactly to the release of one mol of H_2O per mol of complex (Calcd. 2.5%); the relatively low temperature of water loss shows that these water molecules are crystal lattice held.[11,36] Another endothermic decomposition occurs between 230 and 375 °C, this weight loss is attributed to the loss of two $C_4H_3N_2$ fragments (Calcd. 22.0, Found 21.8%).[11] There are two other TG inflections in the ranges 376 - 428 and 429 - 570 °C, may arise from the elimination of N_2 (Calcd. 3.9, Found 4.1%) and $C_{14}H_{10}O_3$ (Calcd. 31.5, Found 30.9%) fragments, leaving MoO_3 representing (40.9%).

The thermogram of [Pd(Hapdhba)Cl(H_2O)].H_2O is characterized by steps at 25 - 125, 126 - 306, 307 - 405 and 406 - 560 °C regions. The elimination of crystal lattice water (Calcd. 4.6, Found 4.8%),[36] coordinated water (Calcd. 4.6, Found 4.6%), $C_4H_3N_2$ and 1/2Cl_2 (Calcd. 29.2, Found 30.1%),

***Table* 3.** The effect of H_2apdhba concentration on corrosion current density, *Tafel* slops and percentage inhibition of copper in 0.5M HCl at 25 °C

Concentration of H_2apdhba ($moll^{-1}$)	$-E_{corr.}$, mV.	$I_{corr.}$, μA cm^2	β_a, mV dec^{-1}	β_c, mV dec^{-1}	Rp (Ohm cm^2)	θ	%In
0	207.4	1.129×10^{-5}	2.7473	157.8	5.741×10^3	-	-
3×10^{-6}	232.4	5.304×10^{-6}	562.5	227.6	1.327×10^4	0.5302	35.02
5×10^{-6}	247.0	3.742×10^{-6}	436.5	186.5	1.516×10^4	0.6685	66.86
7×10^{-6}	249.4	3.626×10^{-6}	471.4	232.8	1.867×10^4	0.6788	67.88
9×10^{-6}	261.1	1.688×10^{-6}	323.1	146.1	2.588×10^4	0.8505	85.05

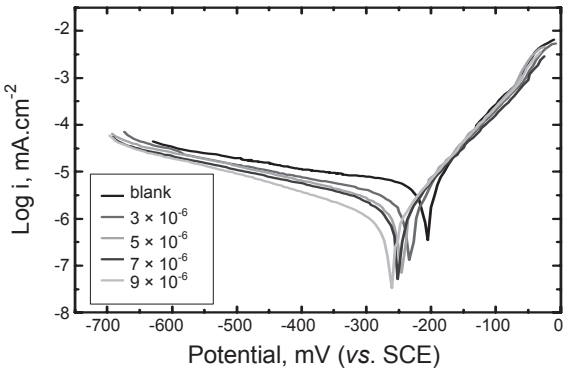

***Fig*. 7.** Potentiodynamic polarization curves of the corossion of Copper in 0.5 M HCl in absence and presence of different concentrations of (H_2apdhba) at 25 °C

C_7H_5O and $1/2N_2$ (Calcd. 30.4, Found 29.9%) fragments, respectively, leaving PdO residue at 700 °C (31.3%).[14]

The thermogram of [Pd(bpy)(Hapdhba)]Cl.H_2O shows four TG inflections in the ranges 32 - 148, 149 - 365, 366 - 480 and 482 - 593 °C. The first weight loss may arise from the elimination of crystal lattice water (Calcd. 3.4, Found 3.8%).[26] The second step may arise from the release of half Cl_2 and $C_4H_3N_2$ fragments (Calcd. 21.6, Found 20.4%), the third step is due to the removal of C_7H_5NO and half bpy (C_5H_4N) fragments (Calcd. 37.2, Found 37.3%),[11,14] while the fourth step is attributed to the removal of the other half of bpy species (Calcd. 14.7, Found 14.5%), followed by the formation of PdO at 680 °C (Calcd. 23.1, Found 24.0%).

Mass spectra

The mass spectrum of H_2apdhba and is in agreement with the assigned formula (*m*/*z* 216; Calcd. 215). The mass spectra of the complexes $[Mo_2O_5(Hapdhba)_2].H_2O$, [Pd(Hapdhba)Cl($H_2O$)].$H_2O$, $[Ru(Hapdhba)_2(H_2O)_2].2H_2O$ and $[Rh(Hapdhba)_2Cl(H_2O)].3H_2O$ are reported and their molecular ion peaks are in agreement with their assigned formulae. The mass spectrum of $[Mo_2O_5(Hapdhba)_2].H_2O$ shows fragmentation patterns corresponding to the successive degradation of the molecule. The first signal at *m*/*e* 719.1 (Calcd. 717.88), in agreement with the molecular ion of the complex, $[Mo_2O_5(Hapdhba)_2]^+$, with 13.6% abundance. The spectrum exhibits signals assigned to step wise ligand loss at *m*/*e* 489, 273 corresponding to $[Mo_2O_5(Hapdhba)]^+$ and $[Mo_2O_5]^+$ fragments, respectively.[26]

The mass spectrum of [Pd(Hapdhba)Cl(H_2O)].H_2O shows fragmentation patterns corresponding to the successive degradation of the complex. The first peak at *m*/*e* 393 with 13.2% abundance represents the molecular ion (Calcd. 391.9). The peaks at 337 and 318 correspond to $[Pd(Hapdhba)(H_2O)]^+$ and $[Pd(Hapdhba)]^+$ fragments, respectively.[33]

The mass spectrum of $[Ru(Hapdhba)_2(H_2O)_2].2H_2O$ shows a signal at *m*/*e* 603 (Calcd. 601.1) with 26.4% abundance. The fragmentation patterns indicates the stepwise ligand loss to $[Ru(Hapdhba)_2]^+$ (531) and $[Ru(Hapdhba)]^+$ (318).[26]

The mass spectrum of $[Rh(Hapdhba)_2Cl(H_2O)].3H_2O$ shows a signal at *m*/*e* 640 (Calcd. 638.4) with 22.2% abundance. The spectrum shows signals at 551, 532, 315 corresponding to $[Rh(Hapdhba)_2(H_2O)]^+$, $[Rh(Hapdhba)_2]^+$ and $[Rh(Hapdhba)]^+$ fragments, respectively.[35]

Electrochemical polarization method

Fig. 7 shows the polarization curves for copper in 0.5M HCl, in presence and absence of the Schiff-base H_2apdhba at different concentrations (3×10^{-6}, 5×10^{-6}, 7×10^{-6}, 9×10^{-6} $molL^{-1}$). The cathodic reaction on copper electrode was inhibited in the presence of H_2apdhba, which was found to affect the cathodic reaction more than the anodic one.[15] This feature is due to the effect of the inhibitor which retards the hydrogen evolution reaction.[15,37] The electrochemical corrosion parameters, i.e., corrosion potential (E_{corr}), cathodic and anodic Tafel slopes and corrosion current (I_{corr}), obtained by extrapolation of Tafel lines, are reported in *Table* 3.

The inhibition efficiency, η_p, was calculated from the equation;

$$\eta_p = [(I_o - I)/I_o] \times 100$$

Where I_o and I are the corrosion current densities in absence and present of inhibitor, respectively.[38]

It is clear that the Schiff-base, H_2apdhba, acts as effective inhibitor. The corrosion inhibition of copper metal is increasing as the inhibitor concentration increase. The maximum inhibition efficiency (85.05%) was obtained at a concentration of 9×10^{-6} molL^{-1} of H_2apdhba.

Acknowledgments. We wish to thank Prof. W. P. Griffith (Chemistry Department, Imperial College of London, UK) for Language corrections and Prof. A. S. Fouda (Chemistry department, Faculty of Science, Mansoura University, Egypt) for his assistance in the potentiodynamic polarization measurements.

REFERENCES

1. Koo, K. K.; Jang, Y. J.; Lee, U. *Bull. Kor. Chem. Soc.* **2003**, *24*, 1014.
2. Jones, R. D.; Summerville, D. A.; Basolo F. *Chem. Rev.* **1979**, *79*, 139.
3. Thangadurai, T. D.; Ihm, S. K. *J. Ind. Eng. Chem.* **2003**, *9*, 563.
4. Thangadurai, T. D.; Ihm, S. K. *J. Ind. Eng. Chem.* **2003**, *9*, 569.
5. Mostafa, S. I.; Ikeda, S.; Ohtani, B. *J. Mol. Cat. A* **2005**, *225*, 181.
6. Dugas, H.; Penney, C. *Bioorganic Chemistry*; Springer: New York 1981, p 435.
7. Khalifa, M. A.; Hassaan, A. M. *J. Chem. Soc. Pak.* **1996**, *18*, 115.
8. Margerum, J. D.; Miller, L. J. *Photochromism*; Wiley Interscience: New York 1971, p 569.
9. Sattari, O.; Alipour, E.; Shirani, S.; Amighian, J. *J. Inorg. Biochem.* **1992**, *45*, 115.
10. Lee, N. H.; Byun, J. C.; Oh, T. H. *Bull. Kor. Chem. Soc.* **2005**, *26*, 454.
11. Sallam, Sh. A.; Ayad, M. I. *J. Kor. Chem. Soc.* **2003**, *47*, 199.
12. Leovac, V. M.; Petrovic, A. F. *Transition Met. Chem.* **1983**, *8*, 337.
13. Hadjikakou, S. K.; Demertzis, M. A.; Kubicki, M.; Kovala-Demertzis, D. *Appl. Organomet. Chem.* **2000**, *14*, 727.
14. Mostafa, S. I.; Badria, F. A. *Met. Based Drug*, **2008**, doi:1155/2008/723634.
15. Ashassi-Sorkhabi, H. A.; Shaabani, B.; Seifzaden, D. *Electrochim. Acta* **2005**, *50*, 3446.
16. Li, S.; Chen, S.; Lei, S. *Corros. Sci.* **1999**, *41*, 1273.
17. Bansiwal, A.; Anthony, P.; Mathur, S. P. *Br Corros. J.* **2000**, *35*, 301.
18. Griffith, W. P.; Mostafa, S. I. *Polyhedron* **1992**, *11*, 871.
19. gaussian 03, Revision B.03, Frisch, M. J.; Trucks, G. W.; Schlegel, H. B.; Scuseria, G. E.; Robb, M. A.; Cheeseman, J. R.; Montgomery, J. A.; Vreven, Jr. T.; Kudin, K. N.; Burant, J. C.; Millam, J. M.; Iyengar, S. S.; Tomasi, J.; Barone, V.; Mennucci, B.; Cossi, M.; Scalmani, G.; Rega, N.; Petersson, G. A.; Nakatsuji, H.; Hada, M.; Ehara, M.; Toyota, K.; Fukuda, R.; Hasegawa, J.; Ishida, M.; Nakajima, T.; Honda, Y.; Kitao, O.; Nakai, H.; Klene, M.; Li, X.; Knox, J. E.; Hratchian, H. P.; Cross, J. B.; Adamo, C.; Jaramillo, J.; Gomperts, R.; Stratmann, R. E.; Yazyev, O.; Austin, A. J.; Cammi, R.; Pomelli, C.; Ochterski, J. W.; Ayala, P. Y.; Morokuma, K.; Voth, G. A.; Salvador, P.; Dannenberg, J. J.; Zakrzewski, V. G.; Dapprich, S.; Daniels, A. D.; Strain, M. C.; Farkas, O.; Malick, D. K.; Rabuck, A. D.; Raghavachari, K.; Foresman, J. B.; Ortiz, J. V.; Cui, Q.; Baboul, A. G.; Clifford, S.; Cioslowski, J.; Stefanov, B. B.; Liu, G.; Liashenko, A.; Piskorz, P.; Komaromi, I.; Martin, R. L.; Fox, D. J.; Keith, T.; Al-Laham, M. A.; Peng, C. Y.; Nanayakkara, A.; Challacombe, M.; Gill, P. M. W.; Johnson, B.; Chen, W.; Wong, M. W.; Gonzalez, C.; Pople, J. A.; *Gaussian, Inc., Pittsburgh PA*, **2003**.
20. Adamo, C.; Barone, V. *J. Chem. Phys.* **1998**, *108*, 664.
21. Becke, A. D. *J. Chem. Phys.* **1993**, *98*, 5648.
22. Geary, W. J. *Coord. Chem. Rev*. **1981**, *7*, 81.
23. Thangadurai, T. D.; Natarajan, K. *Transition Met. Chem*. **2001**, *26*, 717.
24. Thangadurai, T. D.; Natarajan, K. *Synth. React. Inorg. Met.-Org. Chem*. **2001**, *31*, 549.
25. Boudalis, A. K.; Nastopoulos, V.; Perlepes, S. P.; Raptopoulou, C. P.; Terzis, A. *Transition. Met. Chem.* **2001**, *26*, 276.
26. Gabr, I. M.; El-Asmy, H.; Emmam, M. S.; Mostafa, S. I. *Transition Met. Chem.* **2009**, *34*, 409.
27. Nakamoto, K. *Infrared and Raman Sectra of Inorganic and Coordination C*ompounds, 4th ed., Wiley, New York **1986**.
28. Mostafa, S. I. *Transition Met. Chem.* **1998**, *23*, 397.
29. Griffith, W. P.; Mostafa, S. I. *Polyhedron* **1992**, *11*, 2997.
30. Maurya, M. R.; Jayaswal, M. N.; Puranik, V. G.; Chakrabarti, P.; Gopinathan, S.; Gopinathan, C. *Polyhedron,* **1997**, *16*, 3977.
31. Bhattacharyya, D.; Chakraborty, S.; Munshi, P.; Lahiri, G. K. *Polyhedron* **1999**, *18*, 2951.
32. Pesce, B. *Nuclear Magnetic Resonance in Chemistry*, Academic Press: New York 1965, p 174.
33. Mostafa, S. I. *Transition Met. Chem.* **2007**, *32*, 769.
34. Li, Y. T.; Jan, C. W.; Zheng, Y. J.; Liao, D. Z. *Polyhedron* **1998**, *17*, 1423.
35. Mostafa, S. I. *J. Coord. Chem.* **2008**, *61*, 1553.
36. Mostafa, S. I.; Perlepes, S. P.; Hadjiliadis, N. *Z. Naturforsch.* **2001**, *56b*, 394.
37. Lagrene, M.; Mernari, B.; Bouanis, M.; Traisnel, M.; Bentiss, F. *Corros. Sci.* **2002**, *44*, 573.
38. Shahin, M.; Bilgic, S.; Yilmaz, H. *Appl. Surf. Sci.* **2003**, *1*, 195.